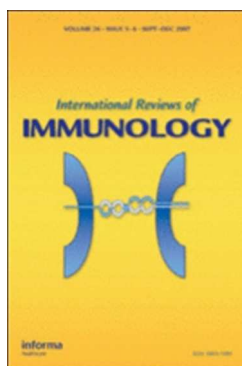


Application of camelid heavy-chain variable domains (VHHs) in prevention and treatment of bacterial and viral infections.

WILKEN, L., MCPHERSON, A.

2018

This is an original manuscript / preprint of an article published by Taylor & Francis in International Reviews of Immunology on 28/11/2017, available online: <http://www.tandfonline.com/10.1080/08830185.2017.1397657>



Application of camelid heavy-chain variable domains (VHHs) in prevention and treatment of bacterial and viral infections

Journal:	<i>International Reviews of Immunology</i>
Manuscript ID	GIRI-2017-0034.R1
Manuscript Type:	Review
Date Submitted by the Author:	16-Aug-2017
Complete List of Authors:	Wilken, Lucas; Robert Gordon University, School of Pharmacy and Life Sciences; Hochschule Bonn-Rhein-Sieg - Campus Rheinbach, Department of Natural Sciences McPherson, Anne; Robert Gordon University, School of Pharmacy and Life Sciences
Keywords:	nanobodies, immunotherapy, single-domain antibody, infectious disease

SCHOLARONE™
Manuscripts

1
2
3
4
5
6
7
8
9
10
11
12
13
14
15
16
17
18
19
20
21
22
23
24
25
26
27
28
29
30
31
32
33
34
35
36
37
38
39
40
41
42
43
44
45
46
47
48
49
50
51
52
53
54
55
56
57
58
59
60

1 Lucas Wilken^{1,2,*}, Anne McPherson¹

2 **Application of camelid heavy-chain variable domains (VHHs) in**
3 **prevention and treatment of bacterial and viral infections**

4
5 ¹School of Pharmacy and Life Sciences, Robert Gordon University, Garthdee
6 Road, Aberdeen, AB10 7GJ, United Kingdom; ²Department of Natural
7 Sciences, Hochschule Bonn-Rhein-Sieg, Von-Liebig-Straße 20, 53359
8 Rheinbach, Germany.

9
10 *Corresponding author: Lucas Wilken. E-mail: l.wilken@rgu.ac.uk.

28 **Abstract**

29 Camelid heavy-chain variable domains (VHHs) are the smallest, intact, antigen-
30 binding units to occur in nature. VHHs possess high degrees of solubility and
31 robustness enabling generation of multivalent constructs with increased avidity –
32 characteristics that mark their superiority to other antibody fragments and monoclonal
33 **antibodies**. Capable of effectively binding to molecular targets inaccessible to classical
34 immunotherapeutic agents and easily produced in microbial culture, VHHs are
35 considered promising tools for pharmaceutical biotechnology. With the aim to
36 demonstrate the perspective and potential of VHHs for the development of
37 prophylactic and therapeutic drugs to target diseases caused by bacterial and viral
38 infections, this review article will initially describe the structural features that underlie
39 the unique properties of VHHs and explain the methods currently used for the
40 selection and recombinant production of pathogen-specific VHHs, and then thoroughly
41 summarise the experimental findings of five distinct studies that employed VHHs as
42 inhibitors of host–pathogen interactions or neutralisers of infectious agents. Past and
43 recent studies suggest the potential of camelid heavy-chain variable domains as a
44 **novel modality** of immunotherapeutic drugs and a promising alternative to monoclonal
45 antibodies. VHHs demonstrate the ability to interfere with bacterial pathogenesis by
46 preventing adhesion to host tissue and sequestering disease-causing bacterial toxins.
47 To protect from viral infections, VHHs may be employed as inhibitors of viral entry by
48 binding to viral coat proteins or blocking interactions with cell-surface receptors. The
49 implementation of VHHs as immunotherapeutic agents for infectious diseases is of
50 considerable potential and set to contribute to public health in the near future.

51

52 **Key words:** nanobodies, immunotherapy, single-domain antibody, infectious disease

53

54

55 **Introduction**

1
2
3 56 **Structure and properties of VHHs**
4

5 57 The production and secretion of pathogen-specific antibodies by plasma B lymphocytes
6
7 58 forms an integral part of the adaptive immune response to microbial infections in
8
9 59 vertebrates. Immunoglobulin G (IgG) is the most abundant antibody type in serum
10
11 60 and constitutes for about 75 % of circulating antibodies. Due to its great availability,
12
13 61 IgG is used as the principal antibody in immunological research. It is composed of two
14
15 62 identical light chains and two identical heavy chains connected by disulphide bridges
16
17 63 [1,2].

18
19
20 64 Apart from conventional IgG glycoproteins with normal antibody assembly,
21
22 65 sera of *Camelidae* were found to contain a high abundance of IgG subclasses, i.e. IgG₂
23
24 66 and IgG₃, devoid of light chains. Moreover, these heavy-chain-only antibodies lack the
25
26 67 constant heavy chain 1 domain (C_H1) which causes direct connection of their heavy
27
28 68 chain variable domain (V_H) to the hinge. The camelid heavy-chain variable domain
29
30 69 exhibits general structural features of a conventional V_H, but is unique in its amino
31
32 70 acid sequence, and therefore denoted as VHH [3].

33
34 71 Equivalent to conventional V_Hs, VHHs consist of four framework regions (FRs)
35
36 72 separating the three complementarity determining regions (CDRs) (or hypervariable
37
38 73 regions) that are involved in antigen binding. VHHs are fully functional for antigen
39
40 74 binding and their binding affinities are not affected by the absence of light chains.
41
42 75 Moreover, the repertoire of antigen-binding sites is increased due to broadly size-
43
44 76 distributed CDRs with diverse amino acid patterns. Particularly, CDR3 of VHHs
45
46 77 distinguishes itself from CDR3 of conventional V_Hs by higher variability of its amino
47
48 78 acid residues. CDR3 is on average longer and parts of this region that, in conventional
49
50 79 IgG, associate with the light chain variable domain (V_L) are available for antigen
51
52 80 binding in VHHs. These features improve antigen recognition and binding strength,
53
54 81 and thus compensate for the absence of the V_L, which normally accounts for half of
55
56 82 the antigen-binding surface. Furthermore, the presence of Cys residues in CDR1 and
57
58 83 CDR3 enables the formation of disulphide bridges that stabilise the structure of the
59
60 84 antigen-binding site [4–6].

1
2
3 85 VHH domains are the smallest, naturally occurring, antigen-binding units with a
4
5 86 molecular weight of 15 kDa [7]. Their small size allows for rapid penetration of tissues
6
7 87 and enables construction of engineered multivalent formats with higher avidity than
8
9 88 monoclonal antibodies (mAbs) and other antigen-binding units [8]. Moreover,
10
11 89 solubility is notably increased in VHHs due to the presence of hydrophilic amino acid
12
13 90 residues in FR2. Hence, these antibody fragments are resistant to aggregation and
14
15 91 their monomeric nature is preserved in solution [9].

16
17
18 92 Amino acid substitutions cause considerable reshaping of the VHH surface [10]
19
20 93 resulting in a large structural diversity of VHH paratopes, e.g. cavity, protruding loop
21
22 94 and flat surface. Thereby, the binding of epitopes inaccessible to mAbs, such as those
23
24 95 located in the active site of enzymes, is enabled [11].

25
26 96 Their small size, variability, stability, avidity and solubility characteristics
27
28 97 render VHHs promising tools for immunotherapy.

29
30 98

31 32 99 **Selection and production of VHHs**

33
34 100 In order to obtain pathogen-specific VHHs for drug development, their generation
35
36 101 must be artificially induced in an experimental host. For this purpose, camelids are
37
38 102 immunised with a particular antigen isolated from the infectious organism. Peripheral
39
40 103 blood (PB) is collected from which PB lymphocytes are prepared by density gradient
41
42 104 centrifugation. The cells are lysed and mRNA is isolated. Extracts of mRNA are used as
43
44 105 templates for cDNA synthesis by reverse transcription polymerase chain reaction (RT-
45
46 106 PCR). In a "nested" approach, Ig heavy chains are amplified with gene-specific
47
48 107 primers. Reamplification of VHH genes with specialised primer sets that introduce
49
50 108 restriction endonuclease (RE) recognition sites at the 5' and 3' ends of the RT-PCR
51
52 109 products enables precise RE digestion of VHH cDNAs [12] which are then processed
53
54 110 for screening by phage, ribosome or yeast display [13]. For phage display, the most
55
56 111 common of display technologies, digested products are cloned into the bacteriophage
57
58 112 coat protein gene present in phagemid vectors [14]. The resulting recombinant DNA
59
60 113 molecules are transformed into competent bacterial cells for gene expression.

1
2
3 114 Bacterial cells are cultured to high density before infected with a helper phage [12],
4
5 115 which provides packaging functions for phagemids, and thus, promotes phage particle
6
7 116 formation plus their secretion into culture medium [15]. Thereby, a library of
8
9 117 phagemid virions, each expressing a different VHH as fusion with their coat protein, is
10
11 118 constructed. In a selection process, i.e. panning, VHH-displaying phage clones are
12
13 119 applied to microtitre wells coated with the specific antigen. Adsorption of phage
14
15 120 particles on the immobilised antigen, due to antigen-antibody interaction, is revealed
16
17 121 by an indirect enzyme-linked immunosorbent assay (ELISA) using horseradish
18
19 122 peroxidase-conjugated secondary antibodies directed against the phage coat protein.
20
21 123 Vector DNA from positively selected clones is then introduced into *Escherichia coli* for
22
23 124 bacterial production, with yields between 3 and 6 mg L⁻¹ [12].

25
26 125 For increased cost efficiency, VHH fragments may be alternatively generated in
27
28 126 lower eukaryotic organisms, esp. yeasts, as these are less fastidious and more
29
30 127 productive, with secretion levels above 250 mg L⁻¹. For this purpose, cDNA encoding
31
32 128 the selected VHH is ligated into an episomal yeast expression vector. Cellular entities
33
34 129 of *Saccharomyces cerevisiae* or *Pichia pastoris* are transformed with the recombinant
35
36 130 vector and the pathogen-specific VHH is produced by fermentation [16,17].

37
38 131 Subsequently, purified expressed products are subjected to antibody specificity
39
40 132 and affinity testing by ELISA methods [12], in order to assess their suitability for
41
42 133 further *in vitro* or *in vivo* studies.
43
44

45 134

46 135 **VHHs directed against bacterial pathogens**

47 136 **Treatment of dental caries**

48
49 137 Insufficient oral care, in combination with a high-sugar diet, augments the
50
51 138 development of diverse biofilm communities on tooth surfaces, i.e. the formation of
52
53 139 dental plaque. Acidic conditions and adhesion sites, provided by the dental plaque,
54
55 140 favour the growth of the oral pathogen *Streptococcus mutans* on tooth surfaces. *S.*
56
57 141 *mutans* further decreases pH by the production of acidic compounds from fermentable
58
59
60

1
2
3 142 carbohydrates. Thereby, severe damage is caused to tooth enamel resulting in tooth
4
5 143 decay, which is symptomatic of dental caries [18–20].
6

7 144 Adherence of *S. mutans* to the salivary pellicle is mediated by the cell surface
8
9 145 streptococcal antigen (SA) I/II [21]. Prevention of adhesin–receptor interactions could
10
11 146 therefore assist in the removal of *S. mutans* from tooth surfaces. In 2006, Krüger *et*
12
13 147 *al.* developed an immunotherapeutic approach for the treatment of caries in patients
14
15 148 with hyposalivation that uses llama VHHs targeted against SA I/II.
16

17 149 Krüger *et al.* (2006) constructed a VHH antibody library from PB lymphocytes
18
19 150 of llamas immunised with disrupted and intact *S. mutans* HG982. Screening for llama
20
21 151 VHH directed against *S. mutans* yielded an antibody specific to SA I/II, denoted S36-
22
23 152 VHH [20]. Previous studies had shown that coupling of VHH to enzymes enhances
24
25 153 their therapeutic effect [22]. Therefore, by linkage of the selected VHH and *Aspergillus*
26
27 154 *niger*-derived glucose oxidase (GOx), a fusion protein (S36-VHH-GOx) was formed to
28
29 155 enhance the salivary peroxidase system (SPS) [20]. When glucose and oxygen are
30
31 156 available, GOx produces hydrogen peroxide (H₂O₂), which is required by peroxidase to
32
33 157 oxidise the salivary components iodide (I⁻) and thiocyanate (SCN⁻) to the antibacterial
34
35 158 compounds hypiodite (OI⁻) and hypothiocyanite (OSCN⁻) [23]. Genes encoding S36-
36
37 159 VHH and S36-VHH-GOx were ligated into *S. cerevisiae* expression vectors and
38
39 160 produced as described previously [16]. ELISAs demonstrated that the fusion of GOx to
40
41 161 S36-VHH had no negative effect on the binding of SA I/II [20].
42
43

44 162 Therapeutic effects of these VHHs on cariogenesis were further assessed *in*
45
46 163 *vivo*. For this purpose, the clinical situation in patients with hyposalivation was
47
48 164 simulated by a desalivated rat model. In order to establish a basis for cariogenesis,
49
50 165 rats received a diet high in sucrose and were repeatedly infected with *S. mutans* NG8.
51
52 166 After three weeks, rats were administered with a single dose of either VHH per day.
53
54 167 Both, S36-VHH and S36-VHH-GOx, were found to decrease colonisation with *S.*
55
56 168 *mutans* and to exert an anticariogenic effect, however, not to statistically significant
57
58 169 degrees. Furthermore, no additional therapeutic effect of GOx in the S36-VHH-GOx
59
60 170 fusion protein was observed. Its nonappearance was believed to result from heavy

1
2
3 171 plaque accumulation, partial inhibition of enzyme activity by the prevailing low pH as
4
5 172 well as the lack of the electron acceptor oxygen within the plaque [20].
6

7 173 Although postulated, the SPS could not be enhanced. Due to virtual absence of
8
9 174 saliva, the GOx substrate glucose was scarce, which resulted in minimal H₂O₂
10
11 175 generation. Consequently, the amount of oxidisable substrate, i.e. I⁻ or SCN⁻, was
12
13 176 limited leading to considerably low antibacterial effects. Krüger *et al.* (2006) suggest
14
15 177 administering a mixture of S36-VHH-GOx, lactoperoxidase, and I⁻ or SCN⁻, in case of
16
17 178 hyposalivation, to achieve a bactericidal effect of the SPS.
18
19
20 179

21 22 180 **Reduction of lipopolysaccharide toxicity**

23
24 181 Lipopolysaccharide (LPS), or endotoxin, is a constituent of the outer membranes of
25
26 182 gram-negative bacteria. When released into the blood stream after infection, it causes
27
28 183 an acute inflammatory response with detrimental effects to organs and tissues, a
29
30 184 condition described as sepsis. Sepsis results from the interaction of LPS with high-
31
32 185 affinity LPS receptor complexes present on cells of the immune system and in plasma,
33
34 186 which induces the release of interleukin 8 (IL-8) and other inflammatory cytokines
35
36 187 [24–26].
37

38
39 188 An important cause of sepsis (and meningitis) is the gram-negative pathogen
40
41 189 *Neisseria meningitidis* [27]. Meningococcal LPS is classified into twelve distinct
42
43 190 immunotypes (L1 to L12) based on structural diversity of the outer core – a result of
44
45 191 phase variation [28,29]. Albeit the heterogeneous structures of meningococcal LPS, its
46
47 192 lipid A moiety and inner-core regions exhibit considerable conservation among gram-
48
49 193 negative bacteria [30].
50

51 194 Protection against a variety of gram-negative bacteria could therefore be
52
53 195 provided by immunotherapy targeting these conserved LPS components [31].
54

55 196 Prerequisites for the efficient use of antibodies in the prevention of sepsis comprise
56
57 197 the recognition of an epitope located in the conserved inner core of the LPS molecule
58
59 198 and the ability to compete with cell surface LPS receptor complexes. El Khattabi *et al.*
60
199 explored the potential of anti-LPS VHHs for sepsis therapy in 2006.

1
2
3 200 From PB lymphocytes of llamas, El Khattabi *et al.* (2006) generated a
4
5 201 nonimmune, i.e. without immunisation of the animal, VHH phage display library. Four
6
7 202 VHH-displaying phages that specifically bound to LPS immunotype L3 from the *N.*
8
9 203 *meningitidis* strain H44/76 were selected, and purified anti-LPS VHHs were
10
11 204 subsequently produced. All VHHs were found to immunoprecipitate meningococcal LPS
12
13 205 forms, while some VHHs additionally reacted with LPS of other gram-negative
14
15 206 pathogens (*E. coli* B4:O111, *Salmonella enterica* serovar Typhimurium and *Bordetella*
16
17 207 *pertussis*). Epitope mapping was performed to determine the binding sites of the anti-
18
19 208 LPS VHHs. It was revealed that one anti-LPS VHH (VHH 5G) bound within the lipid A
20
21 209 and KDO regions of an *rfaC* mutant strain, while the other three reacted with an LPS-
22
23 210 deficient mutant strain (*lpxA*) for unknown reasons.
24
25

26 211 The effect of anti-LPS VHH on the binding of meningococcal L3 LPS by LPS
27
28 212 receptors on innate immune cells was investigated and it was demonstrated that L3
29
30 213 LPS–receptor interactions could be efficiently blocked in the presence of VHH 5G.
31
32 214 Furthermore, it was studied whether effector cell response to LPS could be prevented
33
34 215 by VHH 5G. LPS was effectively sequestered by VHH 5G inhibiting the release of
35
36 216 proinflammatory molecules. In addition, LPS depletion due to immunoprecipitation by
37
38 217 anti-LPS VHHs was assessed to be sufficient for the detoxification of solutions
39
40 218 contaminated with LPS [32].
41
42

43 219 With VHH 5G, an antibody was isolated that recognises LPS from different
44
45 220 gram-negative bacteria when present in their outer membranes and in a purified, free
46
47 221 form. VHH 5G is able to disturb interactions between LPS and its receptors, disrupt
48
49 222 corresponding signalling pathways that normally generate sepsis-related effector
50
51 223 molecules, and deplete LPS from aqueous solutions with high efficiency.
52

53 224

54 225

55 226

56 227 **Prevention of enterotoxigenic *E. coli*-induced post-weaning diarrhoea**
57
58
59
60

1
2
3 228 Enterotoxigenic *E. coli* (ETEC) strains are causative of human and porcine morbidity
4
5 229 and mortality [33] as these bacteria express heat-labile and heat-stable enterotoxins
6
7 230 that cause ionic imbalance and secretory type diarrhoea in infected subjects [34,35].
8
9 231 ETEC virulence is determined, *inter alia*, by F4 fimbriae, which are filamentous protein
10
11 232 appendages that interact with F4-specific receptors (F4Rs) present on the epithelium
12
13 233 of the small intestine, and thereby mediate the intestinal colonisation by ETEC [36].
14
15 234 Intestinal isolates of ETEC from piglets with post-weaning diarrhoea (PWD) – a cause
16
17 235 of absent maternal immunity [37] – exhibit prevalence of the serological variant F4ac
18
19 236 [38]. In 2005, Harmsen *et al.* aimed to use monoclonal VHHs, raised against ETEC
20
21 237 F4ac fimbriae, for PWD immunotherapy.

22
23
24 238 Harmsen *et al.* (2005) isolated F4ac fimbriae from the F4 positive (F4+) ETEC
25
26 239 strain CVI-1000, which is devoid of F5, F6, F17, F18 and F41 fimbriae, and used these
27
28 240 to immunise a llama and recover its VHH repertoire from PB lymphocytes. Yeast VHH
29
30 241 expression libraries were created whence six clones, directed against the F4 fimbriae
31
32 242 major subunit, were selected. Two clones did not significantly inhibit bacterial
33
34 243 attachment to jejunal brush borders and displayed cross-reactivity with other F4
35
36 244 variants, whereas four VHHs that specifically recognised the F4ac fimbrial variant
37
38 245 prevented F4+ ETEC attachment. The llama VHH K609 showed the strongest inhibitory
39
40 246 activity and was therefore subjected to further studies.

41
42
43 247 First, small intestinal segments of F4R positive (F4R+) piglets, i.e. piglets with
44
45 248 brush borders that bound above six ETEC per unit, were perfused with solutions of
46
47 249 ETEC and different concentrations of K609. Net fluid absorption was measured to
48
49 250 determine the effect of VHHs on ETEC-induced fluid loss. Perfusion with K609 at 4 mg
50
51 251 L⁻¹ accounted for maximal reduction of ETEC-induced fluid loss, however, only to
52
53 252 about 30 %. Second, faecal dry matter content was analysed in two groups of weaned
54
55 253 piglets with severe diarrhoea, evoked by the oral challenge with porcine rotavirus
56
57 254 strain RV277 and the ETEC strain CVI-1000. Subjects of the experimental group were
58
59 255 orally administered daily with either low or high doses of K609, while the control
60
256 group received no treatment. Faecal dry matter content of the group treated with

1
2
3 257 K609 was higher compared to control piglets, but statistical significance of this
4
5 258 difference was merely recorded for piglets administered with high doses. Overall,
6
7 259 reduction of diarrhoea was poor and improvement of piglet mortality was insignificant.

8
9 260 Possible errors that may have contributed to the limited effectivity of K609
10
11 261 immunotherapy have been suggested. These include degradation of K609 by
12
13 262 proteases of the gastrointestinal tract and the expression of adhesion factors, other
14
15 263 than F4 fimbriae, by the ETEC strain CVI-1000. Furthermore, intestinal colonisation of
16
17 264 ETEC expressing other fimbrial types or F4 variants cannot be prevented by K609
18
19 265 alone, owing to its specificity. It is rather suggested to produce a mixture of VHHs
20
21 266 directed against various ETEC adhesion factors, in order to effectively obviate PWD
22
23 267 [39].
24
25
26
27

28 269 **VHHs directed against viruses**

30 270 **Treatment of human respiratory syncytial virus infection**

31
32
33 271 Human respiratory syncytial virus (RSV) is the main contributor to lower respiratory
34
35 272 tract infection (LRTI) in infants [40]. Patients who encountered RSV-induced
36
37 273 bronchiolitis or pneumonia during infancy are at increased risk of developing asthma
38
39 274 and chronic obstructive pulmonary disease in adulthood [41,42]. RSV specifically
40
41 275 infects the apical membrane of ciliated respiratory epithelial cells [43] and triggers
42
43 276 clinical symptoms of LRTI after a short incubation period [44].
44

45 277 RSV pathogenesis is promoted by virulence factors, esp. the envelope
46
47 278 glycoproteins G and F, encoded by a linear single-stranded, nonsegmented, negative-
48
49 279 sense RNA molecule [45]. The G protein mediates viral attachment to epithelial cell
50
51 280 receptors [46], whereas the F protein induces the fusion of viral and epithelial cell
52
53 281 membrane which enables the entry of the RSV ribonucleoprotein into host cell
54
55 282 cytoplasm [47]. Furthermore, the F protein evokes the fusion of infected cells with
56
57 283 adjacent cells to form multinucleated cells (syncytia) [48].
58

59 284 RSV is classified into two subgroups, i.e. subgroup A (RSV-A) and subgroup B
60
285 (RSV-B), based on antigenic variation of the G protein [49]. In contrast, high

1
2
3 286 conservation has been identified in the amino acid sequence of the F protein [50]. The
4
5 287 development of therapeutic agents specifically targeting the F protein could therefore
6
7 288 be highly valuable in the inhibition of viral entry. A trivalent VHH, specific to the RSV F
8
9 289 protein, was recently designed and characterised by Detalle *et al.* (2016) and
10
11 290 subjected to a functional comparison with its monovalent form and the prophylactic
12
13 291 anti-RSV mAb palivizumab [51].

14
15
16 292 Llama immune libraries were generated by injection with soluble recombinant F
17
18 293 protein, inactivated RSV-A or a combination of the two. A monovalent VHH specific to
19
20 294 the RSV F protein (Nb017) was identified from the library. Three units of Nb017 were
21
22 295 additionally formatted into a trivalent VHH, denoted ALX-0171, using flexible GS
23
24 296 linkers. Both RSV-neutralising VHHs were readily produced in a *P. pastoris* strain.

25
26 297 Assessment of the binding to the RSV F protein, by surface plasmon resonance
27
28 298 analysis, revealed that both ALX-0171 and Nb017 bind its pre-fusion conformation,
29
30 299 where the trimeric format exhibited a marked increase in binding affinity.
31
32 300 Furthermore, the effect of trimeric formatting on RSV neutralisation capacity was
33
34 301 determined by microneutralisation assays. The potency of the trivalent ALX-0171
35
36 302 against RSV-A and RSV-B strains was found to be several thousandfold higher than
37
38 303 that of the monovalent Nb017. Moreover, a significant increase in potency, as
39
40 304 compared to palivizumab, was ascertained.

41
42
43 305 The capabilities of ALX-0171 and palivizumab to completely suppress RSV
44
45 306 replication were compared at equivalent concentrations. ALX-0171 caused complete
46
47 307 blockage of virus replication in 87 % of viruses tested, whereas palivizumab reduced
48
49 308 viral titres by only 18 %. By studying the binding to RSV mutants with alterations in
50
51 309 antigenic site II or IV of the RSV F protein, it was demonstrated that ALX-0171
52
53 310 specifically targets antigenic site II. Furthermore, it was observed that ALX-0171
54
55 311 partially competes with palivizumab for the binding of the RSV F protein which
56
57 312 suggests **overlap** of their epitopes.

58
59 313 As Detalle *et al.* (2016) intended to administer ALX-0171 by nebulisation, it
60
314 was determined whether the nebulisation process causes aggregation, fragmentation

1
2
3 315 or reduced potency of ALX-0171. Higher- and lower-molecular-weight species were
4
5 316 detected at minimum levels, but ALX-0171 potency remained unaffected.
6

7 317 The *in vivo* efficacy of ALX-0171 against RSV was studied in cotton rats. ALX-
8
9 318 0171 was administered at different doses either by nebulisation before or intranasally
10
11 319 after RSV challenge. Viral loads in the nose and lungs were significantly reduced for all
12
13 320 doses of intranasally administered ALX-0171. Delivered prophylactically via
14
15 321 nebulisation, ALX-0171 reduced nasal RSV titres in a dose-dependent matter and in
16
17 322 the lungs it completely blocked RSV replication, even at the lowest dose tested (1 mg
18
19 323 kg⁻¹). ALX-0171 is therefore superior to palivizumab, which had no effect on viral
20
21 324 titres at doses lower than 15 mg kg⁻¹.
22
23

24 325 ALX-0171 is a potential therapeutic VHH that specifically and efficiently binds
25
26 326 antigenic site II of the RSV F protein. In comparison to Nb017 and palivizumab, ALX-
27
28 327 0171 distinguishes itself by increased neutralisation capacity and inhibition efficiency,
29
30 328 which are a result of its trivalency. Moreover, administration by nebulisation enables
31
32 329 direct delivery of ALX-0171 to the site of infection and hence a faster exertion of its
33
34 330 antiviral effect [52].
35

36 331 In May 2016, positive results for ALX-0171 in Phase I/IIa clinical trials were
37
38 332 reported by the Belgian biopharmaceutical company Ablynx [53].
39
40

41 333

42 334 **Eradication of poliovirus-induced infantile paralysis (poliomyelitis)**

43
44 335 Poliomyelitis, or infantile paralysis, is a highly contagious disease caused by infection
45
46 336 with poliovirus (PV) [54]. Three distinct serotypes, PV1, PV2 and PV3, all of which
47
48 337 cause paralytic disease, have been identified based on differences in their antigenic
49
50 338 determinants [55]. The single-stranded positive sense RNA genome of PV [56] is
51
52 339 enclosed in a non-enveloped capsid composed of 60 monomers of four different
53
54 340 polypeptides, i.e. viral protein 1 (VP1), VP2, VP3 and VP4 [57], that are arranged in
55
56 341 icosahedral symmetry [58]. PV recognises and binds CD155, a transmembrane
57
58 342 glycoprotein of the Ig superfamily [59]. Extracellular domains of CD155 interact with a
59
60 343 conserved narrow surface depression in the PV capsid, termed canyon [60], inducing a

1
2
3 344 conformational change of the virion that initiates cell entry and uncoating [61,62]. In
4
5 345 rare cases, PV reaches the central nervous system where it replicates in motor
6
7 346 neurons of the spinal cord and thereby causes muscle paralysis [63].
8

9
10 347 Prophylactic treatment by inactivated polio vaccine (IPV) [64] and oral polio
11
12 348 vaccine [65] led to near eradication of poliomyelitis [66]. Other treatment options
13
14 349 such as mAb 35-1f4, which neutralises PV1 by virion cross-linking [67], and the
15
16 350 capsid-binding pyridazinamine analogue R75761 [68] have been developed. In 2010,
17
18 351 Thys *et al.* isolated and characterised VHHs specific to PV1 and assessed their antiviral
19
20 352 activity *in vitro*.
21

22 353 By repeated infection of a dromedary with PV1 Sabin strain and isolation of its
23
24 354 VHH repertoire, an immune library was created. Fifteen VHH clones that positively
25
26 355 reacted with PV1 Sabin strain in an ELISA were further analysed. In a standard
27
28 356 neutralisation assay their abilities to block infectivity of PV1 (vaccine and wild-type
29
30 357 strain), PV2 and PV3 were determined. Neutralising activity against PV2 and PV3 was
31
32 358 non-existent, whereas both the vaccine and wild-type strain of PV1 were neutralised
33
34 359 by five VHHs (PVSP6A, PVSS8A, PVSP19B, PVSS21E, and PVSP29F). HeLa cell cultures
35
36 360 were incubated with dilutions of these VHHs and cell viability was monitored, in order
37
38 361 to reveal possible cytotoxic effects. Cytotoxicity was, however, not demonstrated for
39
40 362 any of the tested VHHs.
41

42 363 Antiviral activities of the neutralising VHHs at different concentrations were
43
44 364 assessed by examination of their cytopathic reduction effect in HeLa cells infected with
45
46 365 PV1, and were compared with that of mAb 35-1f4 and R75761. Full protection from a
47
48 366 PV1-induced cytopathic effect was provided by PVSP6A and PVSP29F at a
49
50 367 concentration below that of R75761. Moreover, these VHHs exhibited protective
51
52 368 activities comparable to mAb 35-1f4. Among the VHHs tested, the lowest half maximal
53
54 369 effective concentration (EC₅₀) values were obtained for PVSP6A and PVSP29F.
55
56

57 370 In order to further define antiviral activities, abilities of the VHHs to reduce
58
59 371 infectious virus yields were investigated in PV1-infected HeLa cells. Certain
60
372 concentrations of PVSP6A and PVSP29F completely abolished virus replication. In

1
2
3 373 contrast, cells treated with equal concentrations of mAb 35-1f4 showed residual virus
4
5 374 titres.

6
7 375 For the generation of PV1 neutralisation escape mutants, mixtures of PV1 and
8
9 376 VHH were created. Isolation of resistant viruses failed for PVSP6A and PVSP29F due to
10
11 377 complete inhibition of plaque formation. The other three VHHs were unable to
12
13 378 neutralise about 100 plaque forming units (PFU), which was consistent with the
14
15 379 number of PFU expected for a neutralising mAb [69].

16
17 380 Thys *et al.* (2010) aimed to isolate a VHH that could inhibit cellular attachment
18
19 381 and cell entry by binding within the canyon region. Recent studies have demonstrated
20
21 382 that all of the PV1-neutralising VHHs recognise epitopes in the canyon region that
22
23 383 overlap with the binding site for CD155 and thereby block ligand–receptor interactions
24
25 384 [70,71]. Furthermore, PV1 neutralisation escape mutants have been found to bear
26
27 385 amino acid substitutions in capsid VPs closely located to the VHH binding sites [72].

28
29 386 PVSP6A and PVSP29F were the most potent inhibitors of PV1, among the VHHs
30
31 387 tested. Moreover, their efficacies were superior to R75761 and mAb 35-1f4 at
32
33 388 equivalent concentrations. These VHHs could therefore be used to develop advanced
34
35 389 antiviral drugs that prevent or treat PV1-induced poliomyelitis. Additionally, Thys *et al.*
36
37 390 (2010) plan to adapt their immunisation protocols to generate a VHH with protective
38
39 391 activity against all of the three PV types, with the aim to contribute to worldwide
40
41 392 eradication of poliomyelitis.

42
43
44
45 393

46 394 **Conclusions**

47
48
49 395 VHH antibody fragments compare to conventional mAbs in their selectivity, antigen
50
51 396 specificity and binding affinity, **but excel in terms of their small size, robustness and**
52
53 397 **increased solubility, which allow for construction of potent multivalent molecules with**
54
55 398 **high avidity**, and thus are advantageous for the development of therapeutic drugs.
56
57 399 VHHs were found to exceed the *in vivo* efficacies of certain marketed drugs, especially
58
59 400 when assembled into multimeric formats or linked to enzymes. Microbial production of
60
401 VHHs is furthermore a feasible alternative to the generation of mAbs by mammalian

1
2
3 402 cell culture [73] and the chemical synthesis of immunological agents. Albeit the great
4
5 403 pharmaceutical potential, no VHH-based agents have been approved for therapy thus
6
7 404 far. However, some VHHs, such as ALX-0171, are already in advanced clinical phases.
8

9
10 405 Besides their application in prevention and treatment of viral and bacterial
11
12 406 infections, VHHs have been used to combat pathologies such as arthritis [74], cancer
13
14 407 [75] and thrombosis [76], to trace antigens and biomarkers for *in vivo* diagnostic
15
16 408 imaging [77,78], and to protect against lethal scorpion and snake envenoming
17
18 409 [79,80].

19
20 410 Based on their versatile applicability in the biomedical field, VHHs are predicted
21
22 411 as major contributors to the solving of public health problems of the future.
23

24 412

25 413

26 414 **Funding**

27
28
29 415 None to declare.
30

31 416

32 417

33 418 **Declaration of interest**

34
35
36 419 None to declare.
37

38 420

39 421

40 422 **Acknowledgements**

41
42
43 423 None.
44

45 424

46 425

47 426

48 427 **References**

49 428 [1] Padlan EA. Anatomy of the antibody molecule. Mol. Immunol. 1994;31:169–
50

51 429 217.
52
53
54
55
56
57
58
59
60

- 1
2
3 430 [2] Vidarsson G, Dekkers G, Rispens T. IgG subclasses and allotypes: from
4 structure to effector functions. *Front. Immunol.* 2014;5:520.
5
6
7 432 [3] Hamers-Casterman C, Atarhouch T, Muyldermans S, et al. Naturally occurring
8 antibodies devoid of light chains. *Nature.* 1993;363:446–448.
9
10 433
11 434 [4] Muyldermans S, Atarhouch T, Saldanha J, et al. Sequence and structure of VH
12 domain from naturally occurring camel heavy chain immunoglobulins lacking
13 light chains. *Protein Eng.* 1994;7:1129–1135.
14
15
16 436
17
18 437 [5] Harmsen MM, Ruuls RC, Nijman IJ, et al. Llama heavy-chain V regions consist of
19 at least four distinct subfamilies revealing novel sequence features. *Mol.*
20
21
22 438
23
24 439
25
26 440 [6] Vu KB, Arbabi Ghahroudi M, Wyns L, et al. Comparison of Llama VH Sequences
27 from Conventional and Heavy Chain Antibodies. *Mol. Immunol.* 1997;34:1121–
28
29
30 441
31
32 442 1131.
33
34 443 [7] Sheriff S, Constantine KL. Redefining the minimal antigen-binding fragment.
35
36
37 444
38
39 445 [8] Zhang J, Tanha J, Hirama T, et al. Pentamerization of single-domain antibodies
40 from phage libraries: a novel strategy for the rapid generation of high-avidity
41
42
43 446
44
45 447
46
47 448 [9] Chothia C, Gelfand I, Kister A. Structural determinants of immunoglobulin
48 variable domain. *J Mol Biol.* 1998;278:457–479.
49
50
51 449
52
53 450 [10] Desmyter A, Transue TR, Ghahroudi MA, et al. Crystal structure of a camel
54 single-domain VH antibody fragment in complex with lysozyme. *Nat. Struct.*
55
56
57 451
58
59 452
60
453 [11] Desmyter A, Decanniere K, Muyldermans S, et al. Antigen Specificity and High
454 Affinity Binding Provided by One Single Loop of a Camel Single-domain
455
456
457 455
458
459 [12] Arbabi Ghahroudi M, Desmyter A, Wyns L, et al. Selection and identification of
460 single domain antibody fragments from camel heavy-chain antibodies. *FEBS*
461
462
463 457
464
465 458
466
467 459
468
469 456
470
471 457
472
473 458
474
475 459
476
477 457
478
479 458
480
481 457
482
483 458
484
485 457
486
487 458
488
489 457
490
491 458
492
493 457
494
495 458
496
497 457
498
499 458
500

- 1
2
3 459 [13] Harmsen MM, De Haard HJ. Properties, production, and applications of camelid
4 single-domain antibody fragments. *Appl. Microbiol. Biotechnol.* 2007;77:13–22.
5 460
6
7 461 [14] Qi H, Lu H, Qiu H-J, et al. Phagemid Vectors for Phage Display: Properties,
8 Characteristics and Construction. *J Mol Biol.* 2012;417:129–143.
9 462
10
11 463 [15] Rondof S, Koch J, Breitling F, et al. A helper phage to improve single-chain
12 antibody presentation in phage display. *Nat Biotechnol.* 2001;19:75–78.
13 464
14
15 465 [16] Frenken LGJ, Van Der Linden RHJ, Hermans PWJJ, et al. Isolation of antigen
16 specific Llama VHH antibody fragments and their high level secretion by
17 *Saccharomyces cerevisiae*. *J. Biotechnol.* 2000;78:11–21.
18 466
19
20 467
21
22 468 [17] Rahbarizadeh F, Rasaei MJ, Forouzandeh M, et al. Over expression of anti-
23 MUC1 single-domain antibody fragments in the yeast *Pichia pastoris*. *Mol.*
24 469 *Immunol.* 2006;43:426–435.
25 470
26
27 471 [18] Touger-Decker R, Van Loveren C. Sugars and dental caries. *Am J Clin Nutr.*
28 472 2003;78:881S–892S.
29
30
31 473 [19] Forssten SD, Björklund M, Ouwehand AC. *Streptococcus mutans*, caries and
32 simulation models. *Nutrients.* 2010;2:290–298.
33 474
34
35 475 [20] Krüger C, Hultberg A, Marcotte H, et al. Therapeutic effect of llama derived VHH
36 fragments against *Streptococcus mutans* on the development of dental caries.
37 476 *Appl Microbiol Biotechnol.* 2006;72:732–737.
38 477
39
40 478 [21] Russell MW, Lehner T. Characterisation of antigens extracted from cells and
41 culture fluids of *Streptococcus mutans* serotype c. *Arch Oral Biol.* 1978;23:7–
42 479 15.
43 480
44
45 481 [22] Szynol A, De Soet JJ, Sieben-Van Tuyl E, et al. Bactericidal Effects of a Fusion
46 Protein of Llama Heavy-Chain Antibodies Coupled to Glucose Oxidase on Oral
47 482 Bacteria. *Antimicrob. Agents Chemother.* 2004;48:3390–3395.
48 483
49
50 484 [23] Tenovuo J, Pruitt KM. Relationship of the human salivary peroxidase system to
51 oral health. *J Oral Pathol.* 1984;13:573–584.
52 485
53
54 486 [24] Pålsson-McDermott EM, O’Neill LAJ. Signal transduction by the
55 lipopolysaccharide receptor, Toll-like receptor-4. *Immunology.* 2004;113:153–
56 487
57
58
59
60

- 1
2
3 488 162.
4
5 489 [25] Sweet MJ, Hume DA. Endotoxin signal transduction in macrophages. *J Leukoc*
6
7 490 *Biol.* 1996;60:8–26.
8
9 491 [26] Cohen J. The immunopathogenesis of sepsis. *Nature.* 2002;420:885–891.
10
11 492 [27] Rosenstein NE, Perkins BA, Stephens DS, et al. Meningococcal Disease. *N. Engl.*
12
13 493 *J. Med.* 2001;344:1378–1388.
14
15 494 [28] Scholten RJ, Kuipers B, Valkenburg HA, et al. Lipo-oligosaccharide
16
17 495 immunotyping of *Neisseria meningitidis* by a whole-cell ELISA with monoclonal
18
19 496 antibodies. *J. Med. Microbiol.* 1994;41:236–243.
20
21 497 [29] Tsai CM, Boykins R, Frasch CE. Heterogeneity and variation among *Neisseria*
22
23 498 *meningitidis* lipopolysaccharides. *J. Bacteriol.* 1983;155:498–504.
24
25 499 [30] Pollack M, Raubitschek AA, Larrick JW. Human monoclonal antibodies that
26
27 500 recognize conserved epitopes in the core-lipid A region of lipopolysaccharides. *J.*
28
29 501 *Clin. Invest.* 1987;79:1421–1430.
30
31 502 [31] Di Padova FE, Brade H, Barclay GR, et al. A broadly cross-protective monoclonal
32
33 503 antibody binding to *Escherichia coli* and *Salmonella* lipopolysaccharides. *Infect.*
34
35 504 *Immun.* 1993;61:3863–3872.
36
37 505 [32] El Khattabi M, Adams H, Heezius E, et al. Llama Single-Chain Antibody That
38
39 506 Blocks Lipopolysaccharide Binding and Signaling: Prospects for Therapeutic
40
41 507 Applications. *Clin. Vaccine Immunol.* 2006;13:1079–1086.
42
43 508 [33] Berberov EM, Zhou Y, Francis DH, et al. Relative importance of heat-labile
44
45 509 enterotoxin in the causation of severe diarrheal disease in the gnotobiotic piglet
46
47 510 model by a strain of enterotoxigenic *Escherichia coli* that produces multiple
48
49 511 enterotoxins. *Infect. Immun.* 2004;72:3914–3924.
50
51 512 [34] Nataro JP, Kaper JB. Diarrheagenic *Escherichia coli*. *Clin. Microbiol. Rev.*
52
53 513 1998;11:142–201.
54
55 514 [35] Nair B, Takeda Y. The heat-stable enterotoxins. *Microb. Pathog.* 1998;24:123–
56
57 515 131.
58
59 516 [36] Van den Broeck W, Cox E, Oudega B, et al. The F4 fimbrial antigen of

- 1
2
3 517 *Escherichia coli* and its receptors. Vet. Microbiol. 2000;71:223–244.
- 4
5 518 [37] Tzipori S, Chandler D, Smith M, et al. Factors contributing to postweaning
6
7 519 diarrhoea in a large intensive piggery. Aust. Vet. J. 1980;56:274–278.
- 8
9 520 [38] Osek J. Detection of the enteroaggregative *Escherichia coli* heat-stable
10
11 521 enterotoxin 1 (EAST1) gene and its relationship with fimbrial and enterotoxin
12
13 522 markers in *E. coli* isolates from pigs with diarrhoea. Vet. Microbiol. 2003;91:65–
14
15 523 72.
- 16
17 524 [39] Harmsen MM, Van Solt CB, Hoogendoorn A, et al. *Escherichia coli* F4 fimbriae
18
19 525 specific llama single-domain antibody fragments effectively inhibit bacterial
20
21 526 adhesion in vitro but poorly protect against diarrhoea. Vet. Microbiol.
22
23 527 2005;111:89–98.
- 24
25 528 [40] Macasaet FF, Kidd PA, Bolano CR, et al. The etiology of acute respiratory
26
27 529 infections. 3. The role of viruses and bacteria. J. Pediatr. 1968;72:829–839.
- 28
29 530 [41] Backman K, Piippo-Savolainen E, Ollikainen H, et al. Adults face increased
30
31 531 asthma risk after infant RSV bronchiolitis and reduced respiratory health-related
32
33 532 quality of life after RSV pneumonia. Acta Paediatr. 2014;103:850–855.
- 34
35 533 [42] Sikkil MB, Quint JK, Mallia P, et al. Respiratory Syncytial Virus Persistence in
36
37 534 Chronic Obstructive Pulmonary Disease. Pediatr. Infect. Dis. J. 2008;27:S63–
38
39 535 S70.
- 40
41 536 [43] Zhang L, Peeples ME, Boucher RC, et al. Respiratory syncytial virus infection of
42
43 537 human airway epithelial cells is polarized, specific to ciliated cells, and without
44
45 538 obvious cytopathology. J. Virol. 2002;76:5654–5666.
- 46
47 539 [44] Sterner G, Wolontis S, Bloth B, et al. Respiratory syncytial virus. An outbreak of
48
49 540 acute respiratory illnesses in a home for infants. Acta Paediatr. Scand.
50
51 541 1966;55:273–279.
- 52
53 542 [45] Huang YT, Wertz GW. The genome of respiratory syncytial virus is a negative-
54
55 543 stranded RNA that codes for at least seven mRNA species. J. Virol.
56
57 544 1982;43:150–157.
- 58
59 545 [46] Levine S, Klaiber-Franco R, Paradiso PR. Demonstration that Glycoprotein G Is
60

- 1
2
3 546 the Attachment Protein of Respiratory Syncytial Virus. *J. Gen. Virol.*
4
5 547 1987;68:2521–2524.
6
7 548 [47] Walsh EE, Hruska J. Monoclonal antibodies to respiratory syncytial virus
8
9 549 proteins: identification of the fusion protein. *J. Virol.* 1983;47:171–177.
10
11 550 [48] Techaarpornkul S, Barretto N, Peeples ME. Functional analysis of recombinant
12
13 551 respiratory syncytial virus deletion mutants lacking the small hydrophobic
14
15 552 and/or attachment glycoprotein gene. *J. Virol.* 2001;75:6825–6834.
16
17 553 [49] Peret TC, Golub JA, Anderson LJ, et al. Circulation patterns of genetically
18
19 554 distinct group A and B strains of human respiratory syncytial virus in a
20
21 555 community. *J. Gen. Virol.* 1998;79:2221–2229.
22
23 556 [50] Johnson PR, Olmsted RA, Prince GA, et al. Antigenic relatedness between
24
25 557 glycoproteins of human respiratory syncytial virus subgroups A and B:
26
27 558 evaluation of the contributions of F and G glycoproteins to immunity. *J. Virol.*
28
29 559 1987;61:3163–3166.
30
31 560 [51] Impact-RSV Study Group. Palivizumab, a humanized respiratory syncytial virus
32
33 561 monoclonal antibody, reduces hospitalization from respiratory syncytial virus
34
35 562 infection in high-risk infants. *Pediatrics.* 1998;102:531–537.
36
37 563 [52] Detalle L, Stohr T, Palomon C, et al. Generation and Characterization of ALX-
38
39 564 0171, a Potent Novel Therapeutic Nanobody for the Treatment of Respiratory
40
41 565 Syncytial Virus Infection. *Antimicrob. Agents Chemother.* 2016;60:6–13.
42
43 566 [53] Ablynx. Results from the first-in-infant Phase I/IIa study with the anti-RSV
44
45 567 Nanobody, ALX-0171 [Internet]. ALX-0171. 2016 [cited 2016 Nov 23]. Available
46
47 568 from: http://www.ablynx.com/uploads/data/files/ablynx_alx-0171_first-in-
48
49 569 [infant_study_results_webcast_presentation.pdf](http://www.ablynx.com/uploads/data/files/ablynx_alx-0171_first-in-infant_study_results_webcast_presentation.pdf).
50
51 570 [54] Landsteiner K, Popper E. Übertragung der Poliomyelitis acuta auf Affen. *Zeitschr*
52
53 571 *Immunitätsforsch.* 1909;2:377–390.
54
55 572 [55] Bodian D, Morgan IM, Howe HA. Differentiation of types of poliomyelitis viruses;
56
57 573 the grouping of 14 strains into three basic immunological types. *Am. J. Hyg.*
58
59 574 1949;49:234–245.
60

- 1
2
3 575 [56] Kitamura N, Semler BL, Rothberg PG, et al. Primary structure, gene
4 organization and polypeptide expression of poliovirus RNA. Nature.
5 576
6
7 577 1981;291:547-553.
8
9 578 [57] Maizel J V, Summers DF. Evidence for differences in size and composition of the
10 poliovirus-specific polypeptides in infected HeLa cells. Virology. 1968;36:48-54.
11 579
12 580 [58] Hogle JM, Chow M, Filman DJ. Three-dimensional structure of poliovirus at 2.9 Å
13 resolution. Science (80-.). 1985;229:1358-1365.
14 581
15 582 [59] Mendelsohn CL, Wimmer E, Racaniello VR. Cellular receptor for poliovirus:
16 molecular cloning, nucleotide sequence, and expression of a new member of the
17 immunoglobulin superfamily. Cell. 1989;56:855-865.
18 583
19 584 [60] Colston E, Racaniello VR. Soluble receptor-resistant poliovirus mutants identify
20 surface and internal capsid residues that control interaction with the cell
21 receptor. EMBO J. 1994;13:5855-5862.
22 585
23 586 [61] Rossmann MG. Viral cell recognition and entry. Protein Sci. 1994;3:1712-1725.
24 587
25 588 [62] Fricks CE, Hogle JM. Cell-induced conformational change in poliovirus:
26 externalization of the amino terminus of VP1 is responsible for liposome binding.
27 J. Virol. 1990;64:1934-1945.
28 589
29 590 [63] Bodian D. Emerging concept of poliomyelitis infection. Science (80-.).
30 591 1955;122:105-108.
31 592
32 593 [64] Salk JE. Studies in Human Subjects on Active Immunization against
33 Poliomyelitis. I. A Preliminary Report of Experiments in Progress. J. Am. Med.
34 Assoc. 1953;151:1081-1098.
35 594
36 595 [65] Sabin AB. Present status of attenuated live-virus poliomyelitis vaccine. J. Am.
37 Med. Assoc. 1956;162:1589-1596.
38 596
39 597 [66] Nathanson N, Kew OM. From emergence to eradication: the epidemiology of
40 poliomyelitis deconstructed. Am. J. Epidemiol. 2010;172:1213-1229.
41 598
42 599 [67] Thomas AA, Brioen P, Boeyé A. A monoclonal antibody that neutralizes
43 poliovirus by cross-linking virions. J. Virol. 1985;54:7-13.
44 600
45 601 [68] Thys B, De Palma AM, Neyts J, et al. R75761, a lead compound for the
46
47
48
49
50
51
52
53
54
55
56
57
58
59
60

- 1
2
3 604 development of antiviral drugs in late stage poliomyelitis eradication strategies
4
5 605 and beyond. *Antiviral Res.* 2008;78:278–281.
6
7 606 [69] Thys B, Schotte L, Muyldermans S, et al. In vitro antiviral activity of single
8
9 607 domain antibody fragments against poliovirus. *Antiviral Res.* 2010;87:257–264.
10
11 608 [70] Strauss M, Schotte L, Thys B, et al. Five of Five VHHs Neutralizing Poliovirus
12
13 609 Bind the Receptor-Binding Site. *J. Virol.* 2016;90:3496–3505.
14
15 610 [71] Schotte L, Strauss M, Thys B, et al. Mechanism of action and capsid-stabilizing
16
17 611 properties of VHHs with an *in vitro* antipolioviral activity. *J. Virol.*
18
19 612 2014;88:4403–4413.
20
21 613 [72] Schotte L, Thys B, Strauss M, et al. Characterization of Poliovirus Neutralization
22
23 614 Escape Mutants of Single-Domain Antibody Fragments (VHHs). *Antimicrob.*
24
25 615 *Agents Chemother.* 2015;59:4695–4706.
26
27 616 [73] Seifert DB, Phillips JA. The production of monoclonal antibody in growth-
28
29 617 arrested hybridomas cultivated in suspension and immobilized modes.
30
31 618 *Biotechnol. Prog.* 1999;15:655–666.
32
33 619 [74] Coppieters K, Dreier T, Silence K, et al. Formatted anti-tumor necrosis factor α
34
35 620 VHH proteins derived from camelids show superior potency and targeting to
36
37 621 inflamed joints in a murine model of collagen-induced arthritis. *Arthritis Rheum.*
38
39 622 2006;54:1856–1866.
40
41 623 [75] Roovers RC, Laeremans T, Huang L, et al. Efficient inhibition of EGFR signaling
42
43 624 and of tumour growth by antagonistic anti-EFGR Nanobodies. *Cancer Immunol.*
44
45 625 *Immunother.* 2007;56:303–317.
46
47 626 [76] Ulrichs H, Silence K, Schoolmeester A, et al. Antithrombotic drug candidate
48
49 627 ALX-0081 shows superior preclinical efficacy and safety compared with currently
50
51 628 marketed antiplatelet drugs. *Blood.* 2011;118:757–765.
52
53 629 [77] Rothbauer U, Zolghadr K, Tillib S, et al. Targeting and tracing antigens in live
54
55 630 cells with fluorescent nanobodies. *Nat. Methods.* 2006;3:887–890.
56
57 631 [78] Huang L, Gainkam LOT, Caveliers V, et al. SPECT imaging with ^{99m}Tc -labeled
58
59 632 EGFR-specific nanobody for *in vivo* monitoring of EGFR expression. *Mol. Imaging*

- 1
2
3 633 Biol. 2008;10:167–175.
4
5 634 [79] Hmila I, Saerens D, Ben Abderrazek R, et al. A bispecific nanobody to provide
6
7 635 full protection against lethal scorpion envenoming. FASEB J. 2010;24:3479–
8
9 636 3489.
10
11 637 [80] Chavanayarn C, Thanongsaksrikul J, Thueng-in K, et al. Humanized-Single
12
13 638 Domain Antibodies (VH/VHH) that Bound Specifically to *Naja kaouthia*
14
15 639 Phospholipase A2 and Neutralized the Enzymatic Activity. Toxins (Basel).
16
17 640 2012;4:554–567.
18
19
20 641
21
22
23
24
25
26
27
28
29
30
31
32
33
34
35
36
37
38
39
40
41
42
43
44
45
46
47
48
49
50
51
52
53
54
55
56
57
58
59
60